Research Article | Vol. 8, No. 5 | 1 May 2017 | BIOMEDICAL OPTICS EXPRESS 2528

Optics EXPRESS

Using speckle to measure tissue dispersion in optical coherence tomography

CHRISTOS PHOTIOU,[1] EVGENIA BOUSI,[1] IOANNA ZOUVANI,[2] AND COSTAS PITRIS[1,*]

[1]*KIOS Research Center, Department of Electrical and Computer Engineering, University of Cyprus, Nicosia, Cyprus*
[2]*Nicosia General Hospital, Nicosia, Cyprus*
[*]*cpitris@ucy.ac.cy*

Abstract: Tissue dispersion could be used as a marker of early disease changes to further improve the diagnostic potential of optical coherence tomography (OCT). However, most methods to measure dispersion, described in the literature, rely on the presence of distinct and strong reflectors and are, therefore, rarely applicable *in vivo*. A novel technique has been developed which estimates the dispersion-induced resolution degradation from the image speckle and, as such, is applicable *in situ*. This method was verified experimentally *ex vivo* and was applied to the classification of a set of normal and cancerous colon OCT images resulting in 96% correct classification.

OCIS codes: (110.4500) Optical coherence tomography; (260.2030) Dispersion; (100.0100) Image processing.

References and links

1. B. Bouma, G. J. Tearney, S. A. Boppart, M. R. Hee, M. E. Brezinski, and J. G. Fujimoto, "High-resolution optical coherence tomographic imaging using a mode-locked Ti:Al2O3 laser source," Opt. Lett. **20**(13), 1486–1488 (1995).
2. W. Drexler, U. Morgner, F. X. Kärtner, C. Pitris, S. A. Boppart, X. D. Li, E. P. Ippen, and J. G. Fujimoto, "In vivo ultrahigh-resolution optical coherence tomography," Opt. Lett. **24**(17), 1221–1223 (1999).
3. W. Drexler, U. Morgner, R. K. Ghanta, F. X. Kärtner, J. S. Schuman, and J. G. Fujimoto, "Ultrahigh-resolution ophthalmic optical coherence tomography," Nat. Med. **7**(4), 502–507 (2001).
4. G. J. Tearney, B. E. Bouma, and J. G. Fujimoto, "High-speed phase- and group-delay scanning with a gratingbased phase control delay line," Opt. Lett. **22**(23), 1811–1813 (1997).
5. S. Iyer, S. Coen, and F. Vanholsbeeck, "Dual-fiber stretcher as a tunable dispersion compensator for an all-fiber optical coherence tomography system," Opt. Lett. **34**(19), 2903–2905 (2009).
6. L. Froehly, S. Iyer, and F. Vanholsbeeck, "Dual-fibre stretcher and coma as tools for independent 2nd and 3rd order tunable dispersion compensation in a fibre-based 'scan-free' time domain optical coherence tomography," Opt. Commun. **284**(16–17), 4099–4106 (2011).
7. N. Lippok, S. Coen, P. Nielsen, and F. Vanholsbeeck, "Dispersion compensation in Fourier domain optical coherence tomography using the fractional Fourier transform," Opt. Express **20**(21), 23398–23413 (2012).
8. Y. Park, T. Yamauchi, W. Choi, R. Dasari, and M. S. Feld, "Spectroscopic phase microscopy for quantifying hemoglobin concentrations in intact red blood cells," Opt. Lett. **34**(23), 3668–3670 (2009).
9. D. Fu, W. Choi, Y. Sung, Z. Yaqoob, R. R. Dasari, and M. Feld, "Quantitative dispersion microscopy," Biomed. Opt. Express **1**(2), 347–353 (2010).
10. H. Ding, J. Q. Lu, W. A. Wooden, P. J. Kragel, and X. H. Hu, "Refractive indices of human skin tissues at eight wavelengths and estimated dispersion relations between 300 and 1600 nm," Phys. Med. Biol. **51**(6), 1479–1489 (2006).
11. A. J. Levine, G. F. Vande-Woude, W. C. Topp, and J. D. Watson, eds., *Cancer Cells, The Transformed Phenotype* (Cold Spring Harbor, 1984).
12. G. Shetty, C. Kendall, N. Shepherd, N. Stone, and H. Barr, "Raman spectroscopy: elucidation of biochemical changes in carcinogenesis of oesophagus," Br. J. Cancer **94**(10), 1460–1464 (2006).
13. G. P. Agrawal, *Nonlinear Fiber Optics* (Academic Press, 2001), Chap. 3.
14. M. R. Hee, *Optical coherence tomography of the eye* (MIT Thesis, 1997).
15. N. Lippok, S. G. Murdoch, K. L. Wu, and F. Vanholsbeeck, "Dispersion mapping at the micrometer scale using tri-band optical frequency domain imaging," Opt. Lett. **38**(16), 3028–3031 (2013).
16. S. Schlichting, T. Willemsen, H. Ehlers, U. Morgner, and D. Ristau, "Direct in situ GDD measurement in optical coating process," Proc. SPIE **9627**, 96271S (2015).
17. C. Dorrer, N. Belabas, J. P. Likforman, and M. Joffre, "Spectral resolution and sampling issues in Fourier-transform spectral interferometry," J. Opt. Soc. Am. B **17**(10), 1795–1802 (2000).

#279775 https://doi.org/10.1364/BOE.8.002528
Journal © 2017 Received 1 Nov 2016; revised 13 Jan 2017; accepted 2 Feb 2017; published 17 Apr 2017

Optics EXPRESS

18. G. J. Tearney, M. E. Brezinski, J. F. Southern, B. E. Bouma, M. R. Hee, and J. G. Fujimoto, "Determination of the refractive index of highly scattering human tissue by optical coherence tomography," Opt. Lett. **20**(21), 2258–2260 (1995).
19. N. Meitav, E. N. Ribak, and S. Shoham, "Point spread function estimation from projected speckle illumination," Light Sci. Appl. **5**(3), e16048 (2015).

1. Introduction

Wavelength-dependent index of refraction variations are common in many materials giving rise to the phenomenon of dispersion. The result is pulse-width broadening with detrimental effects in applications ranging from communications to imaging. In Optical Coherence tomography (OCT), dispersion mismatch between the two arms of the interferometer causes point spread function (*psf*) broadening and, therefore, a degradation of the resolution. In order to eliminate the consequences of dispersion, several techniques have been developed to compensate for its effects. Traditional compensation methods rely on balancing the dispersion in the two arms of the OCT interferometer by adjusting the type and amount of material in the reference arm. One approach, for example, is to insert a fused-silica prism pair, with faces contacted and index matched, in the reference arm, to form a variable-thickness window. However, this method is usually only practical for compensating dispersion of up to second order [1–3]. Alternatively, grating-based phase delay scanners can also be used for second order dispersion compensation by displacing the diffraction grating from the focal plane of the lens to achieve transform-limited interferogram profiles [4]. Dual optical fiber stretchers have also been employed for dispersion compensation allowing some degree of tunability. Unfortunately, these devices require large and complex hardware and are not very practical [5,6]. Yet another approach is numerical dispersion compensation based on the use of the Fractional Fourier transform (FrFT) which has also served as a visual tool to highlight the physics behind dispersion compensation [7].

While an OCT interferometer can be optimized for its intended purpose, dispersion differences will still emerge due to the variability and diversity of the properties of the tissues that are imaged. Interestingly, since dispersion is specific to the tissue that is causing the effect, it can carry useful information regarding its composition and/or constituent concentration. The concept of exploiting dispersion, as a source of contrast, is not new since there have already been examples of using the dispersion of biomolecules to quantify their concentration. For example, the dispersion of hemoglobin was used to extract the concentration of hemoglobin in intact red blood cell [8]. The relation between dispersion and biochemical composition was further exemplified using quantitative dispersion microscopy, which has confirmed that the dispersion of live HeLa cells agrees well with the dispersion measured for pure proteins solutions [9]. Variations in the dispersion of different types of normal skin have also been identified *in vivo* with coherent reflection measurements of different skin types [10]. Given the dramatic changes in cellular biochemistry caused by cancer [11], which are discernible by other optical techniques such as Raman spectroscopy [12], it is highly likely that dispersion can also be used as a contrast mechanism in OCT imaging. Therefore, Group Velocity Dispersion (GVD) could be used to detect, for example, changes associated with early cancer and result in more accurate disease diagnosis.

Three main methods are described in the literature for estimating the dispersion from OCT images: (i) measuring the degradation of the PSF [13,14], (ii) measuring the shift (walk-off) between images taken at different center wavelengths [15], and (iii) calculating the second derivative of the phase of the spectrum [16,17]. However, these methods require that a strong, distinct, reflector is present in the image which is rarely the case in tissue. In addition, the presence of Mie scattering and speckle can be detrimental to the attempt to measure dispersion.

A new technique for estimating the dispersion is proposed which uses the image speckle to calculate the *psf* degradation and does not rely on distinct and strong reflections. Since speckle is present in most biological samples, this technique is applicable to any tissue and

Optics EXPRESS

can be implemented *in vivo* and *in situ*. The proposed method was verified *ex vivo* and its applicability to cancer diagnosis was evaluated on a small set of gastrointestinal (GI) normal and adenocarcinoma OCT images.

2. Theory and methods

2.1 Estimating the dispersion from the resolution degradation of single reflections

The most straight-forward method to estimate the dispersion is by measuring the broadening of a single reflection's Gaussian envelope. If the original signal has an interferogram width of t_0, the degraded interferogram will have a broader width, t_d, and the two will be related by

$$t_d^2 = t_0^2\left[1+\left(L\cdot GVD\cdot t_0^{-2}\right)^2\right] \tag{1}$$

where L is the sample thickness and GVD is the Group Velocity Dispersion [13,14]. Thus, the GVD can be estimated by:

$$GVD = \sqrt{\left(t_d^2 t_0^2 - t_0^4\right)L^{-2}} \tag{2}$$

In an OCT image, the effects of dispersion are observed as a broadening of the Point Spread Function (*psf*) and, therefore, as a degradation of the resolution. The system resolution, d_0, is defined as the full-width-at-half-maximum (FWHM) of the coherence envelope of a point reflector and is related to the interferogram width, t_0, by

$$t_0 = d_0 \Big/ \left(c\sqrt{4\ln(2)}\right) \tag{3}$$

where c is the speed of light. The same also holds for d_d and t_d, the dispersion-degraded widths. Since the values of d_0 and d_d can be readily measured using OCT, the GVD can be estimated from an OCT image as long as there are distinct point reflectors below and outside the sample. Although this can be arranged *ex vivo* [18], it is rarely the case *in vivo*.

2.2 Estimating the dispersion from the resolution degradation using the image speckle

The previously described methods of dispersion measurement from OCT images are very difficult to apply *in vivo* and are limited only to particular applications where clear and strong, single, reflections are present. The novel method described here can be applied in the absence of such reflectors since the degraded resolution, d_d, is estimated from the dispersion-induced variation of the speckle pattern.

Due to its coherent nature, OCT speckle is also affected by dispersion. The induced change in the speckle size can be used to estimate the image PSF broadening and, subsequently, to calculate the GVD. However, speckle variations, given the randomness of the speckle signal, are difficult to estimate. The approach proposed here is to compare small portions of an OCT image (of the order of twice the width of the system resolution), denoted as $i_s(z)$, which contain mainly speckle. Such a section from the surface of the sample, $i_s(0)$, where there is no dispersion-induced broadening, and one at a depth z, $i_s(z)$, where the effects of dispersion are visible. The two images are related by a depth-dependent speckle-degrading impulse response, $sdf(z)$, such that

$$i_s(z) = sdf(z) * i_s(0) \tag{4}$$

where the * denotes the convolution of the two terms and z, in the solution presented here, takes the values of $z = d_0, 2d_0, \ldots, L$. To obtain an estimate of $sdf(z)$, in a practical and accurate manner, a Wiener-type minimization can be used [19]. For that purpose, the following least mean square error function, $\varepsilon(z)$, is defined

Optics EXPRESS

$$\varepsilon(z) = E\left\{\left|i_s(z) - sdf(z) * i_s(0)\right|^2\right\} \tag{5}$$

where E denotes expectation. Minimizing the error function, $\varepsilon(z)$, using a Wiener deconvolution approach, results in an estimate for $sdf(z)$. In analogy to $sdf(z)$, there exists another impulse response, $rdf(z)$, of a similar form, which describes the dispersion-induced degradation of the system resolution. For calculating the GVD, it is not necessary to explicitly derive the rdf since only its width is required, which can be estimated from

$$d_{rdf}(z) = d_o \frac{d_{sdf}(z)}{d_{sdf}(0)} \tag{6}$$

where d_0 is the system resolution and $d_{sdf}(z)$ is the width of the sdf at depth z. The result of the convolution of the rdf with the OCT image is a degraded image with resolution width $d_d(z)$ given by

$$d_d(z) = \sqrt{(d_0)^2 + \left(d_{rdf}(z)\right)^2} \tag{7}$$

since the convolution of two Gaussians, the psf and the rdf, results also in a Gaussian with a width that is the root mean square of the widths of the two original functions. Given this width, d_d, the GVD can be calculated using Eq. (2).

2.3 Ex vivo verification of the GVD estimate

In order to validate the speckle-based technique, a pure collagen gel and porcine muscle and adipose tissue samples were imaged *ex vivo* and the GVD was estimated using both the standard resolution-degradation method and the novel procedure. The pure collagen samples served the purpose of initially testing the proposed methodology using a sample of known dispersion under well-controlled conditions. In addition, the ex vivo tissue samples served as an initial test of the applicability of the technique to highly scattering biological samples. A swept source OCT system, with a center wavelength of 1300 nm and a resolution of 12 μm in air, was used to image sample sections placed over a reflector (microscope slide) which also served as a reference for the actual thickness and system resolution measurements. Eight images were taken from each different type of sample.

For the purposes of validating the proposed speckle-based method, the GVD was measured using the standard resolution degradation method described in Section A. For each image, the Gaussian width without dispersion (d_0) was measured from the free-space portion of the reflector (i.e. the portion not covered by the sample). The broadened Gaussian width (d_d) was estimated from the width of the reflector below the tissue. Using the location of the glass surface, the actual thickness of the sample (L) was also calculated as the distance from the top surface to the extension of the free-space reflector line (Fig. 1(A)). Given these parameters, the GVD was estimated using Eq. (2) and Eq. (3). In addition, the index of refraction was also calculated, as described in the literature [18]. The thickness of the sample, L, and the additional optical path length delay L', calculated from the OCT images (Fig. 1(A)), were used to get the index of refraction based on the relationship:

$$n = \left(L' + L\right) / L \tag{8}$$

The GVD was also estimated using the speckle-based technique as described in Section B. The median of the GVD from 250 individual A-Scans from each image as well as the standard deviation of the median GVD for all images of each sample type were used to compare the results and evaluate the accuracy of the both methods.

Optics EXPRESS

2.4 Application of the speckle dispersion technique on GI images

To demonstrate the applicability of the novel speckle-based method to human tissues, the technique was applied to OCT images of normal and cancerous colon obtained from patients who were scheduled for surgical excision of their tumors. Eleven normal and 14 abnormal images were included in this preliminary study. Since the actual tissue thickness could not be measured, it was estimated from the distance measured by OCT in air divided by an average index of refraction of 1.4 (which, despite being an approximation, it does not deviate more than 5% from the range reported in the literature). The GVD was estimated up to a depth of approximately 0.5 mm (as measured in air) for 500 A-Scans per image. Using the statistics of these GVD measurements (such as mean, standard deviation, and other moments.) the samples were classified as normal or abnormal using Linear Discriminant Analysis (LDA) and leave-one-out-cross-validation (LOOCV).

3. Results and discussion

The proposed method was initially verified *ex vivo* using a collagen gel and porcine muscle and adipose tissues. Examples of the images collected are shown in Fig. 1 and Fig. 2. The median GVD for each type of sample as well as the standard deviation between the images of each type were calculated as described in Section 2 A and are shown in Table 1.

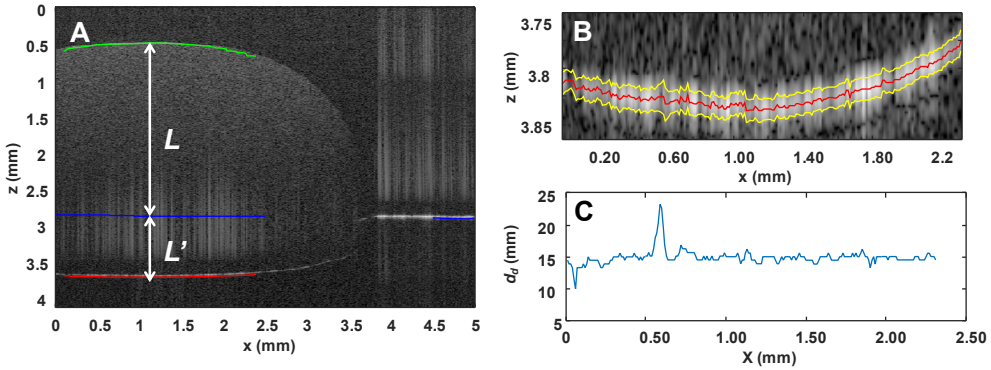

Fig. 1. (A) OCT image of a pure collagen gel placed over a reflector (green line: top surface, red line: bottom surface, blue line: reflector, L: tissue thickness at that particular location). (B) Zoomed portion of the bottom surface (red) with the FWHM (yellow). (C) The FWHM of the reflector calculated at each of 250 A-Scan.

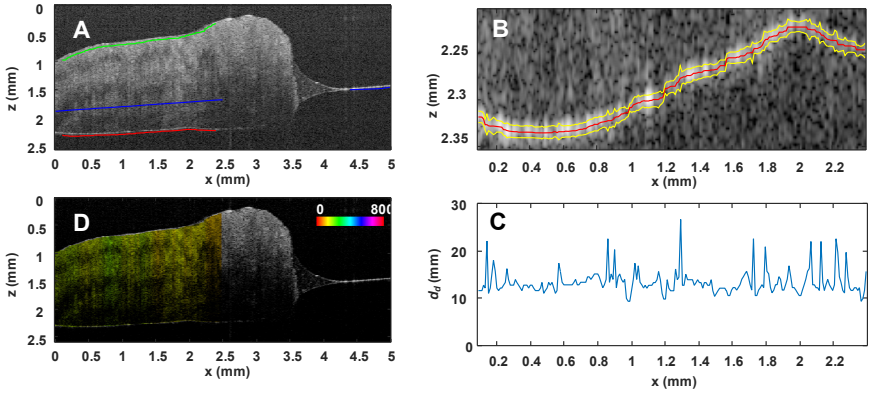

Fig. 2. (A) OCT image of porcine muscle placed over a reflector (green line: top surface, red line: bottom surface, blue line: reflector). (B) Zoomed portion of the bottom surface (red) with the FWHM (yellow). (C) The FWHM of the reflector calculated at each of 250 A-Scan. (D) The OCT image with the GVD overlaid in a pseudo-color hue scale.

Optics EXPRESS

The implementation of the speckle-based approach included the division of each OCT image in smaller strips (twice the width of the system resolution), containing mainly speckle (Fig. 3(A) and 3(B)), and estimating the *sdf* (Fig. 3(C)) with a Wiener-type deconvolution as described before. The width of the *sdf* for all A-Scans was measured and the mean calculated (Fig. 3(D)). The process was repeated as a function of depth (Fig. 3(E)). The dispersion-degraded image resolution width, d_d, was, then, estimated from a linear fit of *sdf* mean width (Fig. 3(F)). This technique was applied to the same samples as the standard method (Fig. 3) and the results were compared to experimentally validate of the new methodology. Table 1 summarizes the results of the GVD measurements using the standard PSF degradation (Section A) and the speckle-based (Section B) techniques. The median GVD values agree within < 7% although the PSF degradation method appears to be slightly more robust with standard deviation of measurements varying between 4 and 12% vs. 9-21%.

Table 1. GVD measured with the PSF degradation and speckle-based methods and mean index of refraction measurements

	PSF degradation method			Speckle-based method			n		
	Median (fs^2/mm)	Std (fs^2/mm)	Std (%)	Median (fs^2/mm)	Std (fs^2/mm)	Std (%)	Median	Std	Std (%)
Collagen	135.72	5.77	4.22	135.62	12.70	9.36	1.369	0.003	0.24
Muscle	136.86	16.79	12.74	133.08	13.59	10.21	1.427	0.032	2.25
Adipose	249.90	28.65	11.68	267.20	55.60	20.81	1.630	0.128	7.70

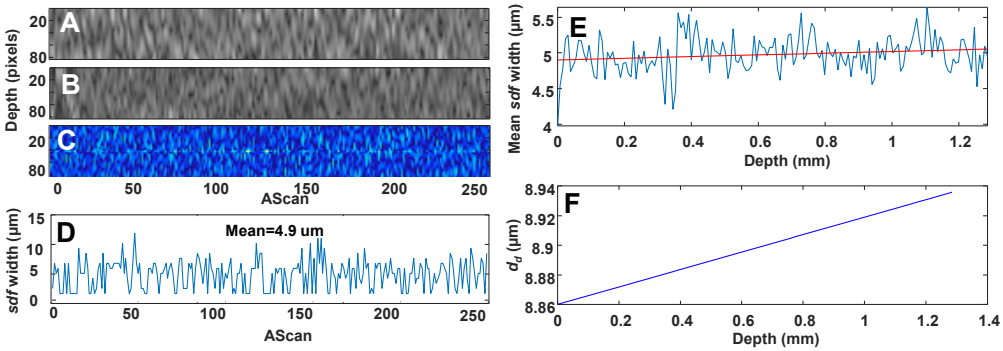

Fig. 3. (A) Portion of the image (80x250 pixels) containing mainly speckle from just below the top surface (z = 0) of the sample of Fig. 1. (B) Similar portion from just above the bottom surface (z = L). (C) The SDF resulting from the deconvolution. (D) The width of the SDF for the 250 A-Scans in (C). (E) The mean SDF width as a function of depth with a linear fit (red line) illustrating the increase as a function of the depth. (F) The degraded width of the PSF as a function of depth calculated from the linear fit in (E).

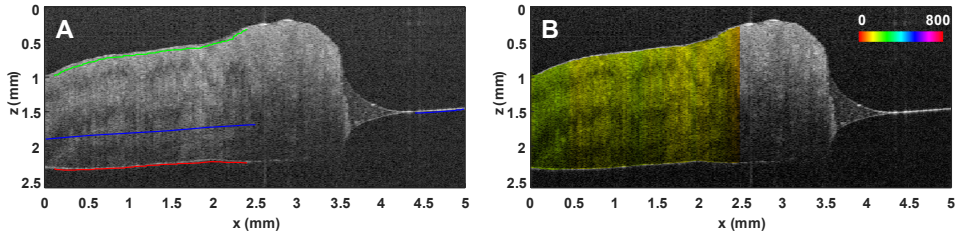

Fig. 4. (A) OCT image of Fig. 1. (D) The OCT image with the GVD, calculated using the speckle-based method, overlaid in a pseudo-color hue scale.

Optics EXPRESS

The GVD was also estimated for the normal and abnormal colon tissues using the speckle-based method (Fig. 4). For each image the moments of the distribution of the GVD values were calculated. Several of these parameters exhibited statistically significant differences with the most significant being the median with a p value of 0.0007 (Fig. 6). A recombination of these parameters using one-way Multivariate Analysis of Variance (MANOVA) for comparing the multivariate means. The resulting canon (C1), i.e. the linear combination of the original variables that has the largest separation between groups, resulted in maximal statistical difference of the two populations. In addition, using the first 6 statistical moments of the GVD values and Linear Discriminant Analysis (LDA) with leave-one-out-cross-validation (LOOCV), the samples were classified with 93% sensitivity and 100% specificity (96% correct classification).

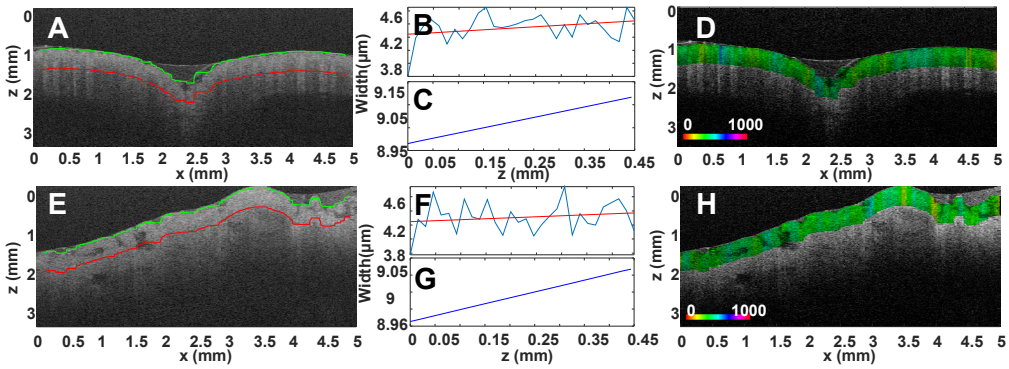

Fig. 5. (A) OCT image of normal colon tissue (green line: top surface, red line: 0.5 mm depth). (B) Mean *sdf* width as a function of depth for (A). (C) Degraded Gaussian width, d_d, as a function of depth calculated from (B). (D) Overlay of the OCT image (gray scale) and the GVD for each A-Scan in a pseudo-color hue scale. (E-H) The same as before for colon adenocarcinoma.

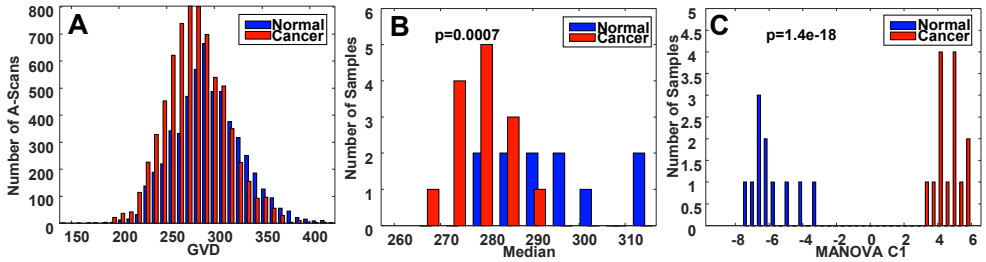

Fig. 6. (A) Distribution of GVD values from normal and abnormal colon. (B) Distribution of the median of the GVD for each image exhibiting statistically significant differences. (C) Recombination of the statistical moments of the GVD values using MANOVA, exhibiting maximal statistical separation.

4. Conclusions

The GVD variations that exist between normal and malignant tissues could be useful in the detection of changes associated with early disease leading to an improvement of the diagnostic utility of OCT. However, most standard techniques to estimate sample dispersion rely on strong and distinct, single, reflections from which the width, shift or phase can be determined. Unfortunately, it is very rare to have such reflections in biological tissues. The new technique, proposed here, can estimate the *psf* degradation from the speckle pattern and is, thus, far more appropriate for *in vivo* imaging. This novel approach was shown, experimentally, to be effective in estimating the GVD with results comparable to the standard technique described in the literature for both low and highly scattering samples. In addition, it

Optics EXPRESS

is sensitive enough to discriminate dispersion changes between normal and cancerous tissues. The success of these preliminary results indicates that further investigation is warranted, which should include both *ex vivo* and *in vivo* validation on a wider range of samples, to further elucidate the advantages and limitations of the proposed technique.

Funding

This research was partially supported by the Research Promotion Foundation of Cyprus and the KIOS Research Center for Intelligent Systems and Networks.